

# Shape Effect on the Reflectance of Sub-Wavelength Structures on Silicon Nitride for Solar Cell Application

Kartik Chandra Sahoo<sup>1</sup>, Yiming Li<sup>1,2,\*</sup> and Edward Y. Chang<sup>3</sup>

<sup>1</sup> Department of Electrical Engineering and Institute of Communications Engineering, National Chiao Tung University, Hsinchu 300, Taiwan; <sup>2</sup> National Nano Device Laboratory, Hsinchu 300, Taiwan

<sup>3</sup> Department of Materials Science and Engineering, National Chiao Tung University, Hsinchu 300, Taiwan

\*Email: ymli@faculty.nctu.edu.tw

## ABSTRACT

We study the spectral reflectivity of conical-, cylindrical- and parabolic-shaped silicon nitride ( $\text{Si}_3\text{N}_4$ ) sub-wavelength structures (SWS). A multilayer rigorous coupled-wave approach is adopted to estimate the reflection properties of  $\text{Si}_3\text{N}_4$  SWS. Optimal shapes of SWS in terms of effective reflectance are analyzed over a range of wavelength. The results of our study show that a 3.15% effective reflectivity could be achieved for the optimized conical-shaped SWS with the height of 160 nm and the non-etched  $\text{Si}_3\text{N}_4$  layer thickness of 70 nm among different shape structure.

**Keywords:** silicon nitride, sub-wavelength structure, shape effect, antireflection coating, multilayer, rigorous coupled-wave approach.

## 1 INTRODUCTION

Polished silicon (Si) surfaces have a high natural reflectivity with a strong spectral dependence. Lowering surface reflectivity of Si by texturization is one of the most important processes for improving the conversion efficiency of Si solar cells and hence various surface texturing techniques has been tried on crystalline silicon. Most used popular texturing technique is RIE technique, which provides high rates of isotropic etching. But, this may form the dislocations and defects in the semiconductor layer [1]. These defects and dislocations are responsible for increasing the minority carrier recombination in solar cell [2]. Thus, the short circuit current for the solar cell is decreased, which in turn decreases the efficiency of solar cell. To reduce the probability of defects creation in the semiconductor layer, sub-wavelength structure (SWS) on anti-reflection coating instead of semiconductor surface has been studied both numerically and experimentally recently [3-5]. Sub-wavelength structure (SWS) on anti-reflection coating surface can improve the efficiency of silicon solar cell. The main motivation for this work was to replace a double layer antireflection coating (ARC) with an antireflective SWS, which can act as a multi-layered ARC with an effective refractive index. The shape of the  $\text{Si}_3\text{N}_4$  SWS studied theoretically earlier was a pyramid shape. The shape of the SWS may be somewhat variable and, therefore,

a multilayer rigorous coupled-wave approach used in [3] is advanced to investigate the reflection properties of silicon nitride ( $\text{Si}_3\text{N}_4$ ) SWS for three different shaped SWS (i.e. parabola, cone and cylinder), assuming a hexagonal nipple lattice.

In this study, a multilayer rigorous coupled-wave approach is advanced to estimate the reflection properties of  $\text{Si}_3\text{N}_4$  SWS. We vary the height of etched part “ $s$ ” and the thickness of non-etched layer “ $h$ ” for three different SWS structures (i.e. parabola, cone, and cylinder) to examine the lowest effective reflectance. The main motivation behind this is to choose optimal shapes of  $\text{Si}_3\text{N}_4$  SWS with the lowest reflectance that can be used in Si solar cell.

## 2 CALCULATION METHOD

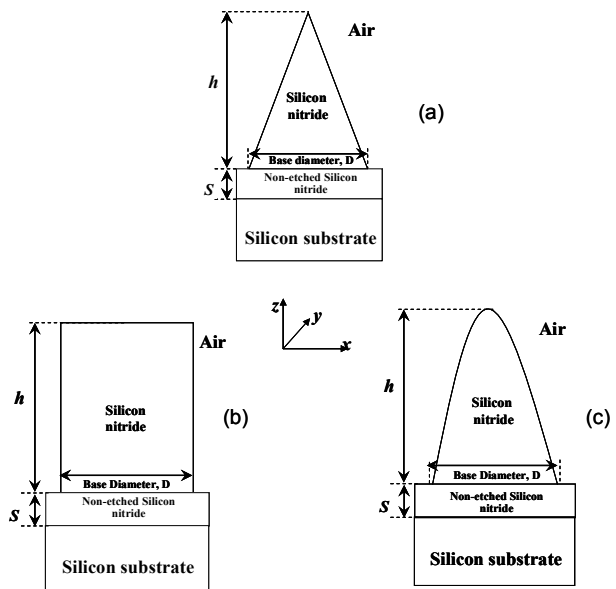


Figure 1: Schematic of two dimensional (2D)  $\text{Si}_3\text{N}_4$  SWS on silicon substrate with  $h$  and  $s$  as designing factors; Shapes of  $\text{Si}_3\text{N}_4$  SWS shown are: (a) Cone, (b) Cylinder, and (c) Parabola.

We study 2D SWS structure with three different shapes (i.e. cone, cylinder and parabola shapes), for the reflectance property with respect to the wavelength. The 2D view of conical-, cylindrical- and parabolic-shaped SWS would look

like the shapes as shown in Fig. 1(a), (b) and (c), respectively. The height of  $\text{Si}_3\text{N}_4$  SWS is  $h$  and the thickness of the non-etched  $\text{Si}_3\text{N}_4$  layer is  $s$ , both of these two parameters are key designing parameters for the reflectance optimization. We use RCWA [3] to study the diffractive structure and its reflectance property, where the effective medium theory (EMT) [6-8] is adopted to calculate the effective refractive index for each partitioned uniform homogeneous layer. We first divide the SWS structure into several horizontal layers with equal thickness and for each discreted position  $z_l$  along the  $z$  direction, EMT implies that the effective refractive index  $n(z_l)$  of each layer is approximated by

$$n(z_l) = \sqrt{\frac{[1 - f(z_l) + n_{\text{SiN}}^2][f(z_l) + (1 - f(z_l))n_{\text{SiN}}^2] + n_{\text{SiN}}^2}{2[f(z_l) + (1 - f(z_l))n_{\text{SiN}}^2]}}, \quad (1)$$

where  $f(z_l)$  is the fraction of  $\text{Si}_3\text{N}_4$  contained in each layer and is given by

$$f(z_l) = \frac{\pi r_l^2}{\sqrt{3}D^2}$$

for conical-, cylindrical- and parabolic-shaped SWS; where  $r_l$  is calculated according to the shape of SWS. The  $r_l$  for parabola-, cone- and cylinder-shaped SWS are given by the following equations, respectively

$$r_l = r \sqrt{\left(1 - \frac{z_l}{h}\right)}, \quad (2)$$

$$r_l = r \left(1 - \frac{z_l}{h}\right), \quad (3)$$

and

$$r_l = r. \quad (4)$$

Notably,  $n_{\text{SiN}} = n + ik$  is the complex refractive index of  $\text{Si}_3\text{N}_4$ ,  $i = \sqrt{-1}$ ,  $n$  and  $k$  are optical constants, and  $n_{\text{air}} = 1$  is the refractive index of air. Only the real part of refractive index of  $\text{Si}_3\text{N}_4$  is considered in our simulation because it is weakly absorbing material [9]. With the calculated effective refractive index  $n(z_l)$  for each layer, we can solve the reflectance property of the entire structure including a layer for the non-etched  $\text{Si}_3\text{N}_4$  with respect to the different wavelengths [3]. Here the incident angle  $\theta$  of sun light is assumed to be normal to the plane (i.e.,  $\theta = 0^\circ$ ), and only the TE polarization is considered here for the calculation of the reflection properties [10].

Instead of considering the reflectance for a certain wavelength, an effective reflectance is computed for the structures over a range of the wavelength of incident sunlight. By taking  $s$  and  $h$  as a varying factor, we calculate the effective reflectance  $R_{\text{eff}}$  [11] for the wavelength  $\lambda$  varying from  $\lambda_l = 400$  nm to  $\lambda_u = 1000$  nm and compare it with  $\text{Si}_3\text{N}_4$  SWS.  $R_{\text{eff}}$  is evaluated by

$$R_{\text{eff}} = \frac{\int_{\lambda_l}^{\lambda_u} \frac{R(\lambda)SI(\lambda)}{E(\lambda)} d\lambda}{\int_{\lambda_l}^{\lambda_u} \frac{SI(\lambda)}{E(\lambda)} d\lambda}, \quad (6)$$

where,  $SI(\lambda)$  is spectral irradiance given by ATM1.5G reference [12],  $E(\lambda)$  is photon energy and  $R(\lambda)$  is the calculated reflection.  $\lambda_l$  and  $\lambda_u$  are the lower and upper wavelength limit, respectively.

### 3 RESULTS AND DISCUSSION

The calculated effective refractive index at  $\lambda = 600$  nm from the top of the SWS to the bottom of  $\text{Si}_3\text{N}_4$  SWS for the four shapes (i.e. parabolic, cone and cylinder) in our simulation is shown in Fig.2. The graded index, which is desirable for suppressing the optical reflection, [13] is observed for cone and parabolic shapes—the refractive index changes from 1.0 to 1.4 for cone and from 1.0 to 1.4 at the air/silicon nitride interface and then changes sharply to the bulk index of silicon nitride. But for a cylinder shaped SWS, the effective refractive index calculated is 1.4. From the comparison, it is found that the slope of the change of refractive index is lowest for cone shaped SWS. Using microwave models, experimentally it has been demonstrated that the strong reflectance reduction by a nipple array with cone-shaped nipples [14]. So it is believed that cone shaped  $\text{Si}_3\text{N}_4$  SWS will give the lowest reflectance compared to parabola or cylinder shaped SWS. The optimizations of the structures and the comparison results will be discussed next.

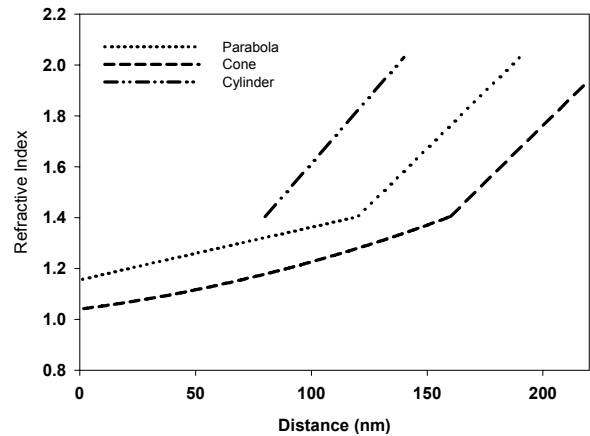


Figure 2: Comparison of the change of calculated effective refractive index at  $\lambda = 600$  nm from the top of the SWS to the bottom of  $\text{Si}_3\text{N}_4$  SWS.

The “ $s$ ” and “ $h$ ” are varied for the studied structures to achieve the lowest effective reflectance and the optimization results are shown in Fig. 2. The reflectance spectra of the optimized structures are compared in Fig. 3.

The lowest effective reflectance of 3.15% is observed for the optimized conical-shaped SWS as compared to the results of pyramid-, cone- and cylinder-shaped structures.

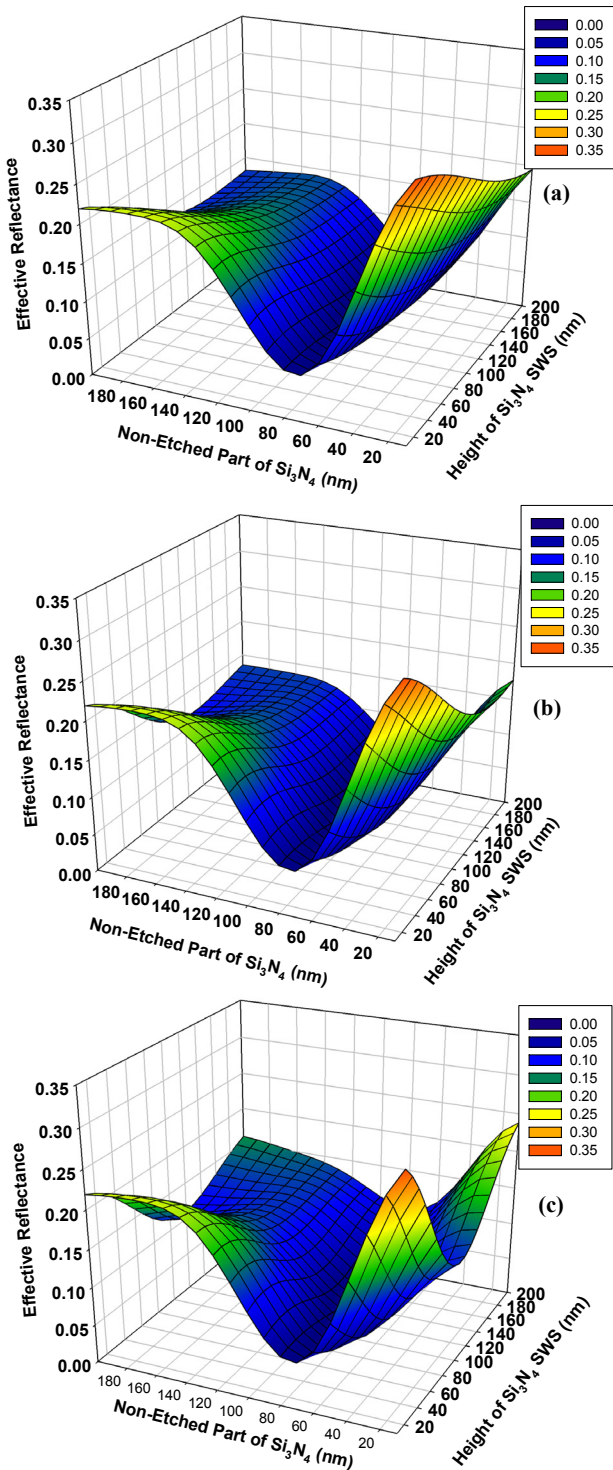


Figure 3: Plot of the effective reflectance for the wavelength varying from 400 nm to 1000 nm; plot is as a function of  $h$  and  $s$  for  $\text{Si}_3\text{N}_4$  SWS for (a) parabolic-, (b) conical-, (c) and cylindrical-shaped structures.

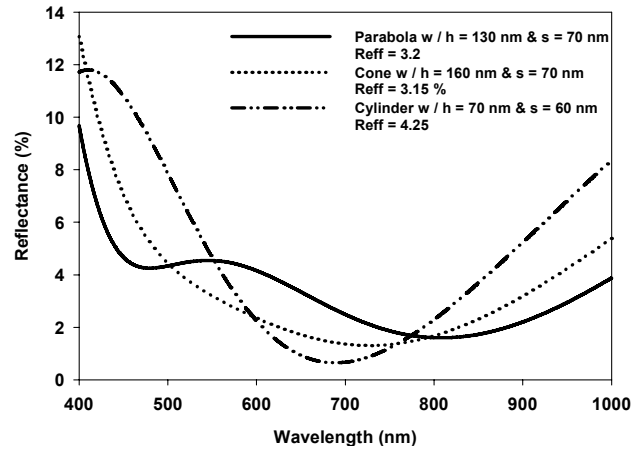


Figure 4: Comparison of the reflectance spectra among the optimized  $\text{Si}_3\text{N}_4$  structures for the wavelength from 400 nm to 1000 nm.

Comparison of the reflectance spectra of the four shapes, as shown in Fig. 4, may not be correct as the volumes of the different shapes are different. For this reason, we keep the volume constant, the thickness of the non-etched  $\text{Si}_3\text{N}_4$  SWS at 70 nm and base diameter ( $D$ ) constant at 80 nm for all shapes. Then the heights of the SWSs were calculated by

$$h = \frac{3V}{\pi \left(\frac{D}{2}\right)^2}, \quad h = \frac{2V}{\pi \left(\frac{D}{2}\right)^2}, \quad h = \frac{V}{\pi \left(\frac{D}{2}\right)^2}$$

for cone, parabola and cylinder shapes, respectively. In the above expressions,  $V$  is represented as volume of SWS. Using the calculated  $h$ , the effective reflectance of all the shapes for a constant volume has been studied for wavelength from 400 nm to 1000 nm. The effective reflectance of the pyramid-, cone-, cylinder-, and parabola-shaped  $\text{Si}_3\text{N}_4$  SWS with different volumes are shown in Fig. 4. For the volume varying from  $1 \times 10^5 \text{ nm}^3$  to  $1 \times 10^6 \text{ nm}^3$ , we find the cone-shaped SWS has the lowest and the cylinder-shaped SWS has the highest effective reflectance, respectively, as compared to other shapes.

Then we varied the base diameter of the three shaped SWS by keeping the volume, and non-etched part ( $s$ ) constant to see the effect on reflectance. Two different volumes (i.e.  $1 \times 10^6/\text{cm}^3$  and  $5 \times 10^6/\text{cm}^3$ ) have been tested in this study. The results are shown in Fig. 6 and it can be seen that in all cases, the cone-shaped SWS has the lowest effective reflectance as compared to other three shaped  $\text{Si}_3\text{N}_4$  SWS studied in this paper.

## 4 CONCLUSIONS

In this paper, we have compared three different shaped silicon nitride sub-wavelength structures. Using the results of rigorous coupled wave analysis simulation for the cone-, cylinder-, and parabola-shaped silicon nitride sub-

wavelength structures, the ratio of silicon nitride sub-wavelength structures height and non-textured part of

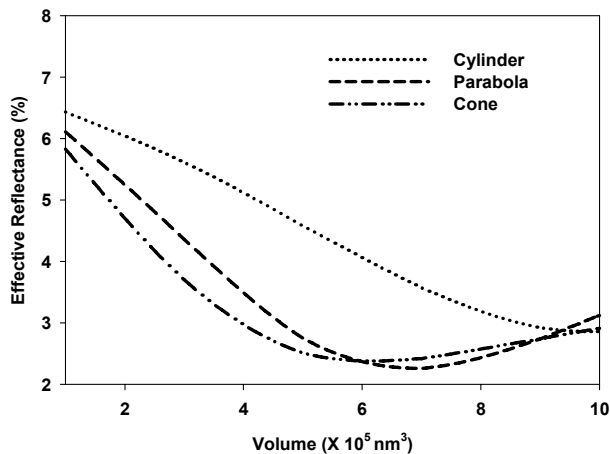


Figure 5: Plot of the effective reflectance with same volume for four different  $\text{Si}_3\text{N}_4$  SWSs for the wavelength varying from 400 nm to 1000 nm.

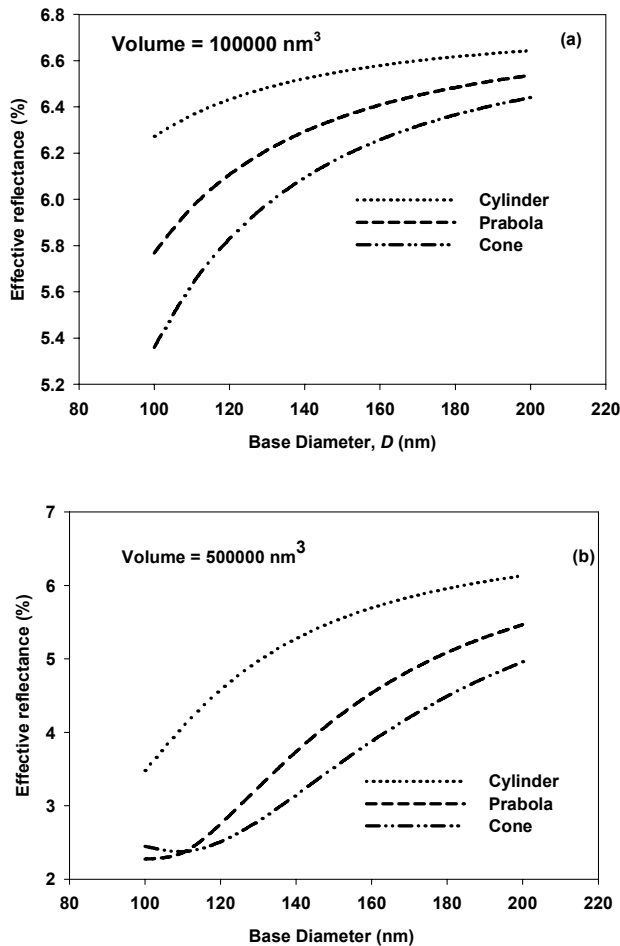


Figure 6: Plot of the effective reflectance with constant volume by varying the base diameter for three different  $\text{Si}_3\text{N}_4$  SWSs for the wavelength varying from 400 nm to 1000 nm.

silicon nitride has been optimized. The reflectance results for the optimized sub-wavelength structures have been compared in terms of effective reflectivity. The lowest effective reflectance of 3.15% is observed for the optimized cone-shaped SWS as compared to the results of parabola- and cylinder-shaped structures. The cone-shaped silicon nitride SWS has been observed to be the best suited for solar cell as compared to the results of cylinder and parabola shapes.

## ACKNOWLEDGEMENT

The work was supported in part by the National Science Council of Taiwan, under Contract NSC-97-2221-E-009-154-MY2 and Contract NSC-98-2120-M-009-010, and by the Chimei-InnoLux Display Corp. Miao-Li, Taiwan under a 2009-2011 grant.

## REFERENCES

- [1] G. Kumaravelu, M. M. Alkaisi, A. Bittar, D. Macdonald, J. Zhao, *Current Appl. Phys.* 4, 108, 2004.
- [2] B. L. Sopori, Y. Zhang, and R. Reedy, in: *Proc. 29<sup>th</sup> IEEE PV Specialists Conference*, 1, 2002.
- [3] K. C. Sahoo, Y. Li, E. Y. Chang, *Comp. Phys. Comm.* 180, 1721, 2009.
- [4] K. C. Sahoo, M. K. Lin, E. Y. Chang, Y. Y. Lu, C. C. Chen, J. H. Huang, and C. W. Chang, *Nanoscale Res. Lett.* 4, 680, 2009.
- [5] K. C. Sahoo, M. K. Lin, E. Y. Chang, T. B. Tinh, Y. Li, and J. H. Huang, *Jpn. J. Appl. Phys.* 48, 1265081, 2009.
- [6] L. Lalanne and M. Hutley, "Artificial media optical properties-subwavelength scale," Dekker, 2003.
- [7] P. Yeh, "Optical Waves in Layered Media," John Wiley & Sons, 1991.
- [8] D. A. G. Bruggeman, *Ann. Phys.* 24, 636-679, 1935.
- [9] J. Zhao, M.A. Green, *IEEE Trans. Electron Dev.* 38, 1925, 1991.
- [10] K. L. Chopra and S. R. Das, "Thin film solar cells," Plenum Press, 1983.
- [11] D. N. Wright, E. S. Marstein and A. Holt, in: *Proc. 31st IEEE Photovoltaic Specialists Conf.*, 1237, 2005.
- [12] <http://rredc.nrel.gov/solar/spectra/am1.5/>
- [13] D. G. Stavenga, S. Foletti, G. Palasantzas, and K. Arikawa, *Proc. R. Soc. London, Ser. B* 273, 661, 2006.
- [14] C. G. Bernhard, W. H. Miller and A. R. Møller, *Acta Physiol. Scand.* 63, 1, 1965.